Phenomenology in minimal cascade seesaw for neutrino mass

刘继元

天津理工大学

Based on RD, ZLH, YL, HJL, JYL, arXiv:1403.2040

Outline

Outline

Neutrino mass — Beyond SM

- There is no neutrino mass in SM.
  No right-handed neutrinos exist in SM.
- Experimental fact from neutrino oscillation:
  - Solar Neutrino Experiment:
    SNO, Homestake, SAGE, GNO, Kamiokande and Super-K, Borexino, $\cdots$
  - Atmospheric Neutrino Experiment:
    Kamiokande-II, Super-K, Soudan-2, MACRO, $\cdots$
  - Accelerator and reactor neutrino experiment:
    LSND, K2K, MINOS, OPERA, T2K, NOνA, KARMEN, MiniBooNE, Chooz, KamLAND, DayaBay, RENO, Double-Chooz, $\cdots$

Neutrino mass — Beyond SM

- There is no neutrino mass in SM.
  No right-handed neutrinos exist in SM.

- Experimental fact from neutrino oscillation:
  - Solar Neutrino Experiment:
    SNO, Homestake, SAGE, GNO, Kamiokande and Super-K, Borexino, $\cdots$
  - Atmospheric Neutrino Experiment:
    Kamiokande-II, Super-K, Soudan-2, MACRO, $\cdots$
  - Accelerator and reactor neutrino experiment:
    LSND, K2K, MINOS, OPERA, T2K, NOνA, KARMEN, MiniBooNE, Chooz, KamLAND, DayaBay, RENO, Double-Chooz, $\cdots$

Neutrino oscillation

PMNS parameterization

$$|\nu_\alpha\rangle = \sum_i V^*_{\alpha i}|\nu_i\rangle, \quad V = U_{\rm PMNS}\cdot {\rm Diag}\{e^{i\rho},\, e^{i\sigma},\, 1\},$$

$$U_{\rm PMNS} = \begin{pmatrix} c_{12}c_{13} & s_{12}c_{13} & s_{13} \\ -c_{12}s_{23}s_{13}-s_{12}c_{23}e^{-i\delta} & -s_{12}s_{23}s_{13}+c_{12}c_{23}e^{-i\delta} & s_{23}c_{13} \\ -c_{12}c_{23}s_{13}+s_{12}s_{23}e^{-i\delta} & -s_{12}c_{23}s_{13}-c_{12}s_{23}e^{-i\delta} & c_{23}c_{13} \end{pmatrix},$$

where $s_{ij} = \sin\theta_{ij},\ c_{ij} = \cos\theta_{ij},\ (ij = 12,\ 23,\ 13)$

Neutrino mass hierarchy patterns

- Normal Hierachy (NH): $m_1 < m_2 < m_3$
- Inverted Hierachy (IH): $m_3 < m_1 < m_2$

Oscillation data

- Global 3ν oscillation analysis (for NH) Fogli *et al.*, 2012

Parameter	Best fit	1σ range	2σ range	3σ range
$\delta m^2/10^{-5}$ eV^2	7.54	[7.32, 7.80]	[7.15, 8.00]	[6.99, 8.18]
$\Delta m^2/10^{-3}$ eV^2	2.43	[2.33, 2.49]	[2.27, 2.55]	[2.19, 2.62]
θ_{12}	33.6°	$[32.6^\circ, 34.8^\circ]$	$[31.6^\circ, 35.8^\circ]$	$[30.6^\circ, 36.8^\circ]$
θ_{23}	38.4°	$[37.2^\circ, 40.0^\circ]$	$[36.2^\circ, 42.0^\circ]$	$[35.1^\circ, 53.0^\circ]$
θ_{13}	8.9°	$[8.5^\circ, 9.4^\circ]$	$[8.0^\circ, 9.8^\circ]$	$[7.5^\circ, 10.2^\circ]$

where $\delta m^2 \equiv m_2^2 - m_1^2$ and $\Delta m^2 \equiv m_3^2 - (m_1^2 + m_2^2)/2$.

Three conventional seesaw models

- The unique, dimension-5 operator is

$$\mathcal{O}_5 = \frac{f_{\alpha\beta}}{\Lambda}\left(\overline{F^C_{L\alpha}}\varepsilon H\right)\left(H^T\varepsilon F_{L\beta}\right),$$ Weinberg, 1979

where $\alpha,\beta = e,\mu,\tau$ and $\varepsilon = i\sigma^2$

- Only three realizations at tree level, Ma, 1998

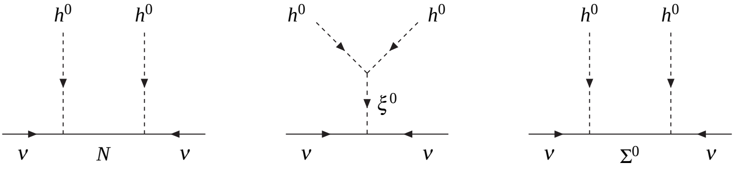

(a) Type I (b) Type II (c) Type III

Beyond conventional seesaws

- Conventional seesaws suffer "seesaw problem":

  large mass of new particles $\longleftrightarrow$ tiny couplings

- Two basic ways to resolve the problem:
  - Heavy particles carry new quantum numbers or discrete symmetries
    — leading mass operators are induced only at the loop level;
  - Heavy particles live in a higher irre. rep. of the SM gauge group
    — seesaw operates through several steps.

Beyond conventional seesaws

- Conventional seesaws suffer "seesaw problem":

  large mass of new particles $\longleftrightarrow$ tiny couplings

- Two basic ways to resolve the problem:
  - Heavy particles carry new quantum numbers or discrete symmetries
    — leading mass operators are induced only at the loop level;
  - Heavy particles live in a higher irre. rep. of the SM gauge group
    — seesaw operates through several steps.

Higher dimension seesaw operators

- Dim-7 seesaw

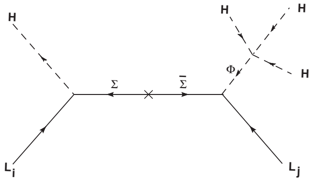

$\Phi \sim (1,4,3),\ \Sigma \sim (1,3,2),$
$\overline{\Sigma} \sim (1,3,-2)$

Babu, et. al., PRD80, 2009

- Dim-9 seesaw

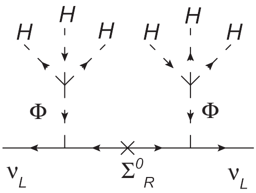

$\Phi \sim (1,4,-1),\ \Sigma_R \sim (1,5,0)$

Kumericki, et. al., PRD86, 2012

Cascade seesaw operator

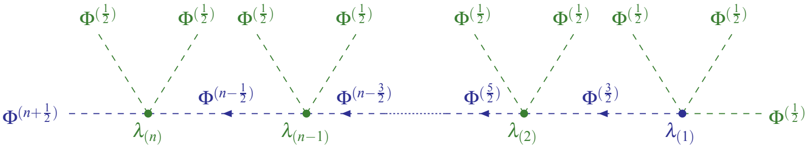

- Dim-$(5+4n)$ operator by a more systematic and economical way.

  Liao, JHEP1106, 2011

- Introducing a heavy fermion multiplet $\Sigma \sim (1, 2n+3, 0)$, neutrino mass is generated by Yukawa coupling $\overline{F_L^C} \Phi^{(n+\frac{1}{2})} \Sigma$.

Outline

Minimal cascade seesaw ($n = 1$)

- New fields: one scalar $\Phi \sim (1,4,1)$ and one fermion $\Sigma \sim (1,5,0)$:

$$\Phi = (\Phi_{+2}, \Phi_{+1}, \Phi_0, \Phi_{-1}), \ \Sigma = (\Sigma_{+2}, \Sigma_{+1}, \Sigma_0, \Sigma_{-1}, \Sigma_{-2})$$

- SM fields: $\phi = (\phi_+, \phi_0)$, $F_L = (\nu_L, \ell_L)$, f_R

Scalars

- Scalar potential:

$$V = -\mu_\phi^2 \phi^\dagger \phi + \lambda_\phi (\phi^\dagger \phi)^2 + \mu_\Phi^2 \Phi^\dagger \Phi$$
$$-\lambda_1 (\Phi\tilde{\Phi})_0 (\phi\tilde{\phi})_0 - \lambda_2 \left((\Phi\tilde{\Phi})_1 (\phi\tilde{\phi})_1\right)_0 + \lambda_3 \left((\Phi\Phi)_1 (\tilde{\Phi}\tilde{\Phi})_1\right)_0 + \lambda_4 \left((\Phi\Phi)_3 (\tilde{\Phi}\tilde{\Phi})_3\right)_0$$
$$-\left[\kappa_1 (\Phi\tilde{\phi}\phi\tilde{\phi})_0 + \text{h.c.}\right] - \left[\kappa_2 \left((\Phi\Phi)_1 (\tilde{\phi}\tilde{\phi})_1\right)_0 + \text{h.c.}\right] - \left[\kappa_3 \left((\Phi\Phi)_1 (\tilde{\Phi}\tilde{\phi})_1\right)_0 + \text{h.c.}\right],$$

where $\tilde{\Phi} = (\Phi^*_{-1}, -\Phi^*_0, \Phi^*_{+1}, -\Phi^*_{+2})$ and $\tilde{\phi} = (\phi^*_0, -\phi^*_+)$

- With the assumptions $\kappa_2 \approx \kappa^2,\ \kappa_1 \approx \kappa_3 \approx \kappa \ll 1$, the minimal of V gives

$$v_\phi \approx \sqrt{\frac{\mu_\phi^2}{2\lambda_\phi}},\ v_\Phi \approx \frac{\kappa v_\phi}{2\sqrt{3} r_\Phi}, \quad \text{where } r_\Phi = \frac{\mu_\Phi^2}{v_\phi^2} + \frac{\lambda_1}{2\sqrt{2}} + \frac{\lambda_2}{2\sqrt{30}}$$

- The mixings between same-charged members of ϕ and Φ are $O(\kappa)$, and the masses of the W and Z bosons are modified by $O(\kappa^2)$ terms

$$m_W \approx \frac{g_2 v_\phi}{\sqrt{2}} \left(1 + \frac{7}{24 r_\Phi^2} \kappa^2\right),\ m_Z \approx \frac{g_2 v_\phi}{\sqrt{2} c_W} \left(1 + \frac{1}{24 r_\Phi^2} \kappa^2\right),$$

Fermions

- By redefining Σ fields,

$$\Sigma^0_{1L} = \frac{1}{\sqrt{2}}(\Sigma_{0L} + \Sigma^C_{0R}),\ \Sigma^0_{2L} = \frac{i}{\sqrt{2}}(\Sigma_{0L} - \Sigma^C_{0R}),$$
$$\Sigma^-_1 = \frac{1}{\sqrt{2}}(\Sigma_{-1} - \Sigma^C_{+1}),\ \Sigma^-_2 = \frac{i}{\sqrt{2}}(\Sigma_{-1} + \Sigma^C_{+1}),$$
$$\Sigma^{--}_1 = \frac{1}{\sqrt{2}}(\Sigma_{-2} + \Sigma^C_{+2}),\ \Sigma^{--}_2 = \frac{i}{\sqrt{2}}(\Sigma_{-2} - \Sigma^C_{+2}),$$

the Yukawa couplings are written as

$$-\mathscr{L}^{\rm Yuk}_{\Phi} = \sum_{m=-2}^{+2} Y^m_{ix}\left[\sqrt{2+m}\,\Phi_m \overline{\Sigma^m_x} P_L \nu_i + \sqrt{2-m}\,\Phi_{m+1}\overline{\Sigma^m_x} P_L \ell_i\right] + \text{h.c.}\ ,$$

where the 3×2 coupling matrices Y^m can be written as,

$$Y^{-2} = Y^{-1} = Y^0 = -Y^{+1} = Y^{+2} = \frac{\sqrt{M_\Sigma}}{\sqrt{2}v_\Phi} Z^*.$$

Parameterization

- $Z = (\mathbf{z}_1, \mathbf{z}_2)$ can be patameterized as ν masses and $U_{\rm PMNS} = (\mathbf{x}_1, \mathbf{x}_2, \mathbf{x}_3)$,

$$\begin{aligned} \text{NH:} \quad & m_{\nu_1} = 0,\ m_{\nu_2} = \lambda_-,\ m_{\nu_3} = \lambda_+, \\ & \mathbf{z}_1 = c_- \mathbf{x}_2 + c_+ \mathbf{x}_3,\ \mathbf{z}_2 = d_- \mathbf{x}_2 + d_+ \mathbf{x}_3, \\ \text{IH:} \quad & m_{\nu_3} = 0,\ m_{\nu_1} = \lambda_-,\ m_{\nu_2} = \lambda_+, \\ & \mathbf{z}_1 = c_- \mathbf{x}_1 + c_+ \mathbf{x}_2,\ \mathbf{z}_2 = d_- \mathbf{x}_1 + d_+ \mathbf{x}_2, \end{aligned}$$

where $c_\pm$, $d_\pm$ can be expressed of $\lambda_\pm$ plus a free complex parameter t,

$$\begin{aligned} c_- &= i\sqrt{\lambda_-}\frac{2t}{1+t^2}, & d_- &= i\sqrt{\lambda_-}\frac{1-t^2}{1+t^2}, \\ c_+ &= i\sqrt{\lambda_+}\frac{1-t^2}{1+t^2}, & d_+ &= -i\sqrt{\lambda_+}\frac{2t}{1+t^2}. \end{aligned}$$

- Details of the model can be found in our paper.

Outline

Radiative transitions

- Diagrams for radiative transitions:

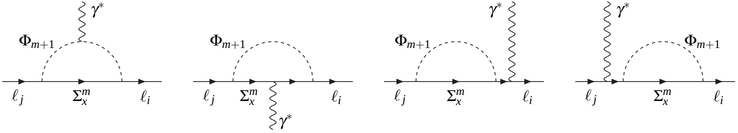

(a) (b) (c) (d)

- The branching ratio for $\ell_j \to \ell_i \gamma$ transition is

$$\mathrm{BR}(\ell_j \to \ell_i \gamma) = \mathrm{BR}(\ell_j \to \ell_i \bar{\nu}_i \nu_j) \times \frac{3\alpha \left|(ZZ^\dagger)_{ij}\right|^2}{64\pi G_F^2 v_\Phi^4 M_\Sigma^2} \left[\sum_{m=-2}^{1} F_m(r)\right]^2,$$

and the anomalous magnetic moment of ℓ_i is

$$a(\ell_i) = \frac{m_i^2 (ZZ^\dagger)_{ii}}{(4\pi)^2 v_\Phi^2 M_\Sigma} \sum_{m=-2}^{1} F_m(r).$$

where $F_m(r)$ are loop functions with $r = M_\Sigma^2 / M_\Phi^2$.

Purely leptonic decays

- Additional box diagram:

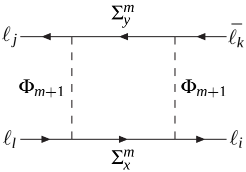

- The branching ratio for $\ell_l \to \ell_i \ell_i \bar{\ell}_i$ transition is

$$\mathrm{BR}(\ell_l \to \ell_i \ell_i \bar{\ell}_i) = \mathrm{BR}(\ell_l \to \ell_i \nu_l \bar{\nu}_i) \frac{1}{2^{13}\pi^4 v_\Phi^4 G_F^2} \left\{ 2 \left| \sum_m (B^m + T_1^m) \right|^2 + \left| \sum_m T_1^m \right|^2 \right.$$

$$\left. -8\mathrm{Re}\left(\sum_m B^m T_2^{m*} \right) - 12\mathrm{Re}\left(\sum_m T_1^m T_2^{m*} \right) + \left[-\frac{8}{3} + 8\ln\frac{m_l^2}{4m_i^2} \right] \left| \sum_m T_2^m \right|^2 \right\},$$

where

$$B^m = -\frac{1}{v_\Phi^2}(ZZ^\dagger)_{il}(ZZ^\dagger)_{ii} H_m(r),$$

$$T_1^m = \frac{e^2 (ZZ^\dagger)_{il}}{M_\Sigma} G_m(r), \quad T_2^m = \frac{e^2 (ZZ^\dagger)_{il}}{M_\Sigma} F_m(r).$$

$\mu - e$ conversion in nuclei

- The $\mu - e$ conversion branching ratio is given by

$$\mathrm{BR}(\mu^- N \to e^- N) = \frac{2|A_R D + \tilde{g}_{LV}^{(p)} V^{(p)} + \tilde{g}_{LV}^{(n)} V^{(n)}|^2}{\omega_{\mathrm{capt}}},$$

where

$$\begin{aligned} A_R &= \frac{\sqrt{2} e (ZZ^\dagger)_{e\mu}}{16(4\pi)^2 v_\Phi^2 M_\Sigma} \sum_m F_m(r), \\ \tilde{g}_{LV}^{(p)} &= 2 g_{LV(u)} + g_{LV(d)} = \frac{\alpha (ZZ^\dagger)_{e\mu}}{\sqrt{2}(4\pi) v_\Phi^2 M_\Sigma} \sum_m G_m(r), \\ \tilde{g}_{LV}^{(n)} &= g_{LV(u)} + 2 g_{LV(d)} = 0, \end{aligned}$$

and overlap integrals D, $V^{(p)}$ and $V^{(n)}$ and ordinary muon capture rate ω_{capt} can be numerically evaluated.

Constraints on LFV transitions

- μ LFV decays

  $\mathrm{BR}(\mu \to e\gamma) < 5.7 \times 10^{-13}$ @ 90% C.L. MEG, 2013

  $\mathrm{BR}(\mu \to 3e) < 1.0 \times 10^{-12}$ @ 90% C.L. SINDRUM, 1988

- $\mu - e$ conversion in nuclei

  $\mathrm{BR}(\mu^- \mathrm{Ti} \to e^- \mathrm{Ti}) < 4.3 \times 10^{-12}$ @ 90% C.L. SINDRUM II, 1993

  $\mathrm{BR}(\mu^- \mathrm{Au} \to e^- \mathrm{Au}) < 7 \times 10^{-13}$ @ 90% C.L. SINDRUM II, 2006

  Future plans: sensitivity will reach $10^{-16} \sim 10^{-18}$

  COMET and PRISM/PRIME at KEK, Mu2e and project-X at Fermilab

- The bound on $\mathrm{BR}(\mu \to e\gamma)$ sets the most stringent constraint.

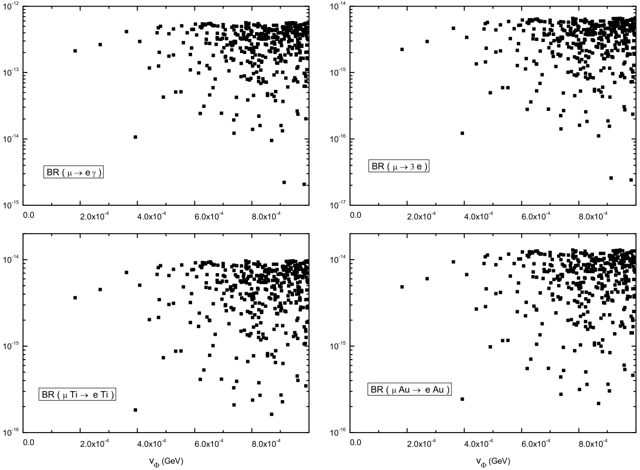

For instance, at $M_\Phi = 200\ \mathrm{GeV},\ M_\Sigma = 300\ \mathrm{GeV}$, $v_\Phi \gtrsim O(10^{-4})\ \mathrm{GeV}$.

Outline

Production

- Tools used for simulation and analysis:
  FeynRules1.7, Madgraph5, Pythia6, PGS, MadAnalysis5, CTEQ6L1...
- Dominant production of new particles at the LHC:
  Drell-Yan process:

$$\begin{aligned} pp &\to \gamma^*/Z^* \to \Phi^*_{+2}\Phi_{+2}/\Phi^*_{+1}\Phi_{+1}/\Phi^*_{-1}\Phi_{-1}/A_0H_0, \\ &\to \gamma^*/Z^* \to \Sigma^{++}\Sigma^{--}/\Sigma^{+}\Sigma^{-}, \end{aligned}$$

  or associated production:

$$\begin{aligned} pp &\to W^* \to \Phi^*_{+1}\Phi_{+2}/A_0\Phi_{+1}/A_0\Phi^*_{-1}/H_0\Phi_{+1}/H_0\Phi^*_{-1}, \\ &\to W^* \to \Sigma^{++}\Sigma^{-}/\Sigma^{+}\Sigma^{0}, \end{aligned}$$

- At 14TeV LHC, $\sigma[\Phi(\Sigma)] \gtrsim 0.01fb$ $(1fb)$ up to a heavy mass of $O(1)$TeV.

Decay property

- Like-sign dilepton decay $\Phi_{+2} \to \ell_i^+ \ell_j^+$ is suppressed, since

$$\frac{\Gamma(\Phi_{+2} \to \ell_i^+ \ell_j^+)}{\Gamma(\Phi_{+2} \to W^+ W^+)} \sim \left(\frac{m_\nu}{M_\Phi}\right)^2 \left(\frac{v_\phi}{v_\Phi}\right)^4 .$$

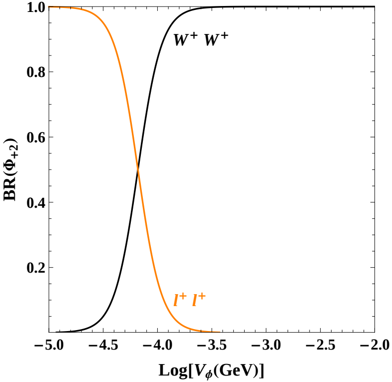

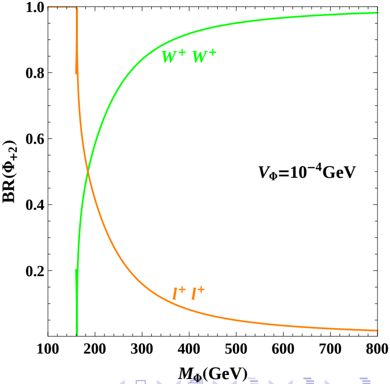

- BRs of Φ in the parentheses at $M_\Phi = 300$ GeV and $v_\Phi = 10^{-2}$ GeV.

	$\Phi^*_{+1} \to b\bar{t}$ (0.32)	$\Phi^*_{+1} \to hW^-$ (0.68)	$\Phi^*_{-1} \to hW^+$ (0.36)	$\Phi^*_{-1} \to ZW^+$ (0.47)
$\Phi_{+1} \to t\bar{b}$ (0.32)	$b\bar{b}t\bar{t}$ (0.10)	$t\bar{b}hW^-$ (0.22)	–	–
$\Phi_{+1} \to hW^+$ (0.68)	$b\bar{t}hW^+$ (0.22)	hhW^+W^- (0.47)	–	–
$\Phi_{-1} \to hW^-$ (0.36)	–	–	hhW^+W^- (0.13)	hZW^+W^- (0.17)
$\Phi_{-1} \to ZW^-$ (0.47)	–	–	hZW^+W^- (0.17)	hhW^+W^- (0.22)
$A_0 \to hZ$ (1.0)	–	–	$hhZW^+$ (0.36)	$hZZW^+$ (0.47)
$H_0 \to W^+W^-$ (0.35)	–	–	$hW^-W^+W^+$ (0.13)	$ZW^-W^+W^+$ (0.17)
$H_0 \to hh$ (0.60)	–	–	$hhhW^+$ (0.22)	$hhZW^+$ (0.28)
$\Phi_{+2} \to W^+W^+$ (1.0)	$b\bar{t}W^+W^+$ (0.32)	$hW^-W^+W^+$ (0.68)	–	–

	$A_0 \to hZ$ (1.0)	$H_0 \to W^+W^-$ (0.35)	$H_0 \to hh$ (0.60)	$\Phi^*_{+2} \to W^-W^-$ (1.0)
$\Phi_{+1} \to t\bar{b}$ (0.32)	$t\bar{b}hZ$ (0.32)	$t\bar{b}W^+W^-$ (0.10)	$t\bar{b}hh$ (0.20)	–
$\Phi_{+1} \to hW^+$ (0.68)	$hhZW^+$ (0.68)	$hW^-W^+W^+$ (0.24)	$hhhW^+$ (0.40)	–
$A_0 \to hZ$ (1.0)	–	hZW^+W^- (0.35)	$hhhZ$ (0.60)	–
$H_0 \to W^+W^-$ (0.35)	hZW^+W^- (0.35)	–	–	–
$H_0 \to hh$ (0.60)	$hhhZ$ (0.60)	–	–	–
$\Phi_{+2} \to W^+W^+$ (1.0)	–	–	–	$W^+W^+W^-W^-$ (1.0)

- BRs of Σ in the parentheses at $M_\Sigma = 300$ GeV and $v_\Phi = 10^{-2}$ GeV.

	$\Sigma^+ \to W^+\nu$ (0.5)	$\Sigma^+ \to h\ell^+$ (0.44)	$\Sigma^+ \to Z\ell^+$ (0.06)	$\Sigma^{++} \to W^+\ell^+$ (1.0)
$\Sigma^0 \to W^\pm\ell^\mp$ (0.5)	$W^\pm W^+\ell^\mp\nu$ (0.25)	$W^\pm h\ell^\mp\ell^+$ (0.22)	$W^\pm Z\ell^\mp\ell^+$ (0.03)	–
$\Sigma^0 \to h\nu$ (0.44)	$W^+h\nu\nu$ (0.22)	$hh\ell^+\nu$ (0.19)	$Zh\ell^+\nu$ (0.026)	–
$\Sigma^0 \to Z\nu$ (0.06)	$W^+Z\nu\nu$ (0.03)	$Zh\ell^+\nu$ (0.026)	$ZZ\nu\nu$ (0.0036)	–
$\Sigma^- \to W^-\nu$ (0.5)	$W^+W^-\nu\nu$ (0.25)	$hW^-\ell^+\nu$ (0.22)	$W^-Z\ell^+\nu$ (0.03)	$W^+W^-\ell^+\nu$ (0.5)
$\Sigma^- \to h\ell^-$ (0.44)	$W^+h\ell^-\nu$ (0.22)	$hh\ell^+\ell^-$ (0.19)	$Zh\ell^+\ell^-$ (0.026)	$W^+h\ell^+\ell^-$ (0.44)
$\Sigma^- \to Z\ell^-$ (0.06)	$W^+Z\ell^-\nu$ (0.03)	$Zh\ell^+\ell^-$ (0.026)	$ZZ\ell^+\ell^-$ (0.0036)	$W^+Z\ell^+\ell^-$ (0.06)
$\Sigma^{--} \to W^-\ell^-$ (1.0)	$W^+W^-\ell^-\nu$ (0.5)	$W^-h\ell^+\ell^-$ (0.44)	$W^-Z\ell^+\ell^-$ (0.06)	$W^+W^-\ell^+\ell^-$ (1.0)

Signal

- Signal channels considered and corresponding processes:

final states	Φ production process in pp collision
$2\ell^\pm 2\ell^\mp$	$\Phi_{+2}\Phi^*_{+2}/A_0 H_0 \to 2\ell^\pm 2\ell^\mp$
$4j2\ell^\pm + \not{E}_T$	$\Phi_{+2}\Phi^*_{+2} \to W^\pm W^\pm W^\mp W^\mp \to jjjj\ell^\pm\ell^\pm\nu\nu$, $\Phi_{+2}\Phi^*_{+1}(\Phi^*_{+2}\Phi_{+1}) \to W^\pm W^\pm + hW^\mp/\bar{t}b(t\bar{b}) \to jjb\bar{b}\ell^\pm\ell^\pm\nu\nu$
$4j2\ell^\pm$	$\Phi_{+2}\Phi^*_{+2} \to \ell^\pm\ell^\pm W^\mp W^\mp \to jjjj\ell^\pm\ell^\pm$, $\Phi_{+2}\Phi^*_{+1}(\Phi^*_{+2}\Phi_{+1}) \to \ell^\pm\ell^\pm + hW^\mp/\bar{t}b(t\bar{b}) \to jjb\bar{b}\ell^\pm\ell^\pm$

final states	Σ production process in pp collision
$2\ell^\pm 2\ell^\mp 2j$	$\Sigma^\pm\Sigma^\mp/\Sigma^0\Sigma^\pm/\Sigma^\pm\Sigma^{\mp\mp} \to hZ(ZZ)\ell^\pm\ell^\mp/W^\pm\ell^\mp Z\ell^\pm/Z\ell^\pm W^\mp\ell^\mp \to jj2\ell^\pm 2\ell^\mp$
$3\ell^\pm\ell^\mp 2j$	$\Sigma^\pm\Sigma^0 \to W^\mp\ell^\pm Z\ell^\pm \to jj3\ell^\pm\ell^\mp$
$3\ell^\pm 2\ell^\mp + \not{E}_T$	$\Sigma^\pm\Sigma^0/\Sigma^{\pm\pm}\Sigma^\mp \to Z\ell^\pm W^\pm\ell^\mp(Z\ell^\pm Z\nu)/W^\pm\ell^\pm Z\ell^\mp \to 3\ell^\pm 2\ell^\mp\nu$
$3\ell^\pm 3\ell^\mp$	$\Sigma^\pm\Sigma^\mp \to \ell^\pm Z\ell^\mp Z \to 3\ell^\pm 3\ell^\mp$

- No. of events of $pp \to \Phi_{+2}\Phi_{+1} \to 4j2\ell^{\pm}$ for $M_{\Phi_{+2},\Phi_{+1}} = 300$ GeV at 14 TeV LHC.

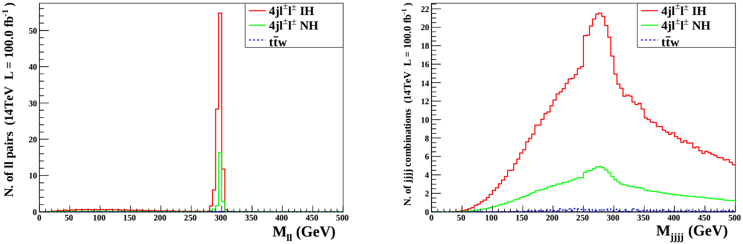

cuts	signal $4j2\ell^{\pm}$		bkg $t\bar{t}W^{\pm}$	$S/\sqrt{S+B}$	
	IH	NH		IH	NH
no cuts	406 (29.7)	81.6 (6)	1409 (124)	9.53 (2.39)	2.11 (0.52)
basic cuts	296.6 (22.5)	60.2 (4.7)	851.3 (81.9)	8.75 (2.2)	1.99 (0.5)
$\not{E}_T < 30$ GeV, $(p_T(\ell), p_T(j)) > (50, 100)$ GeV	212.4 (16.2)	42.7 (3.4)	36.1 (3.2)	13.47 (3.68)	4.81 (1.31)
$60 < M_{jj}/\text{GeV} < 150$ ($M_{W,h}$ reconst.), $280 < M_{ll}/\text{GeV} < 320$	183.1 (13.9)	37.1 (2.9)	1.8 (0.1)	13.47 (3.72)	5.94 (1.67)
$250 < M_{jjjj}/\text{GeV} < 350$	102.6 (7.7)	21.8 (1.7)	0.8 (0.04)	10.09 (2.76)	4.59 (1.27)

- No. of events of $pp \to \Sigma^\pm\Sigma^0 \to 3\ell^\pm 2\ell^\mp + \not{E}_T$ for $M_\Sigma = 300$ GeV at 14 TeV LHC.

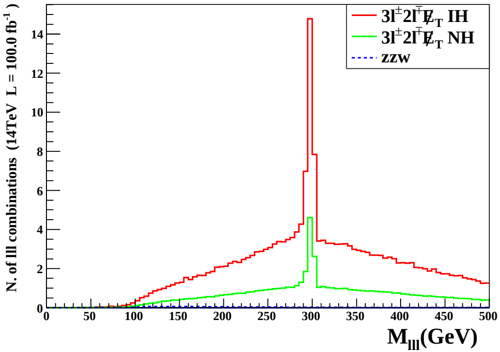

cuts	signal $3\ell^\pm 2\ell^\mp + \not{E}_T$		bkg $ZZW^\pm$	$S/\sqrt{S+B}$	
	IH	NH		IH	NH
no cuts	157 (12.9)	46.5 (3.8)	3 (0.3)	12.4 (3.55)	6.6 (1.87)
basic cuts	51.2 (3.4)	15 (1)	0.7 (0.06)	7.11 (1.84)	3.78 (0.97)

Outline

Conclusions

- The minimal cascade seesaw model is carefully studied in both theoretical and phenomenological aspects including low-energy LFV constraints and LHC signatures.
- The main features and results:
  - A convenient parametrization is used to handle Yukawa couplings.
  - The constraints on LFV transitions are systematically considered. The strictest one comes from the upper bound on the decay $\mu \to e\gamma$, which gives the scalar VEV $v_\Phi \gtrsim O(10^{-4})$ GeV for heavy masses of $200 - 300$ GeV.
  - All relevant decays of new particles are examined for exploring LHC signatures.
    For detecting Φ, the $4j2\ell^\pm$ signal is most important.
    And for Σ, the $2\ell^\pm 2\ell^\mp 2j$, $3\ell^\pm \ell^\mp 2j$ and $3\ell^\pm 2\ell^\mp + \not{E}_T$ signals are quite promising.

Conclusions

- The minimal cascade seesaw model is carefully studied in both theoretical and phenomenological aspects including low-energy LFV constraints and LHC signatures.
- The main features and results:
  - A convenient parametrization is used to handle Yukawa couplings.
  - The constraints on LFV transitions are systematically considered. The strictest one comes from the upper bound on the decay $\mu \to e\gamma$, which gives the scalar VEV $v_\Phi \gtrsim O(10^{-4})$ GeV for heavy masses of $200 - 300$ GeV.
  - All relevant decays of new particles are examined for exploring LHC signatures.

    For detecting Φ, the $4j2\ell^\pm$ signal is most important.

    And for Σ, the $2\ell^\pm 2\ell^\mp 2j$, $3\ell^\pm \ell^\mp 2j$ and $3\ell^\pm 2\ell^\mp + \not{E}_T$ signals are quite promising.

谢 谢 ！